Cripton Peter
First *Last*

ASME Paper Title: Moment Measurements in Spine Segment Dynamic Tolerance Testing using Eccentric Compression are Susceptible to Artifacts Based on Loading Configuration

Authors: Van Toen, C., Carter, J.W., Oxland, T.R., Cripton, P.A.

ASME Journal Title: Journal of Biomechanical Engineering

Volume/Issue 136/12 Date of Publication (VOR* Online) October 31st, 2014

ASME Digital Collection URL: https://asmedigitalcollection.asme.org/biomechanical/article-abstract/136/12/124505/371138/Moment-Measurements-in-Dynamic-and-Quasi-Static

DOI: 10.1115/1.4028817

*VOR (version of record)

Title: Moment Measurements in Spine Segment Dynamic Tolerance Testing using Eccentric Compression are Susceptible to Artifacts Based on Loading Configuration

Authors & Affiliations: Van Toen, C.,[1] Carter, J.W.[2], Oxland, T.R.,[1] Cripton, P.A.[1]

[1]Orthopaedic and Injury Biomechanics Group, Departments of Mechanical Engineering & Orthopaedics and the International Collaboration on Repair Discoveries (ICORD), University of British Columbia, Vancouver BC, Canada

[2]Origin Engineering LLC, Liberty Lake WA, USA

Corresponding Author:

Dr. Peter A. Cripton, Ph.D.

Department of Mechanical Engineering

6250 Applied Science Lane

Vancouver BC

V6T 1Z4

Canada

Phone: 604-822-6629

Fax: 604-822-2403

Email: cripton@mech.ubc.ca

Other Authors :

Ms. Carolyn Van Toen, M.A.Sc.

Orthopaedic and Injury Biomechanics Group, Departments of Mechanical Engineering & Orthopaedics and the International Collaboration on Repair Discoveries (ICORD)

University of British Columbia

818 West 10th Ave, Rm 5000

Vancouver BC

V5Z 1M9

Canada

Phone : 604-675-8845

Fax : 604-675-8849

Email : carolyn@mech.ubc.ca

Dr. Jarrod W. Carter, Ph.D.

Origin Engineering LLC

23403 E. Mission Ave. Suite #223

Liberty Lake WA

99019

Phone: 509-926-2566

Fax: 509-926-2506

Email: jc@oerecon.com

Dr. Thomas R. Oxland, Ph.D.

Orthopaedic and Injury Biomechanics Group, Departments of Mechanical Engineering & Orthopaedics and the International Collaboration on Repair Discoveries (ICORD)

University of British Columbia

818 West 10th Ave, Rm 5460

Vancouver BC

V5Z 1M9

Canada

Phone : 604-675-8834

Fax : 604-675-8849

Email: toxland@interchange.ubc.ca

Word Count: 2,517 (2,500 word limit)

Abstract (418 words, 400 max)

The tolerance of the spine to bending moments, used for evaluation of injury prevention devices, is often determined through eccentric axial compression experiments using segments of the cadaver spine. Preliminary experiments in our laboratory demonstrated that eccentric axial compression resulted in 'unexpected' (artifact) moments. The aim of this study was to evaluate the static and dynamic effects of test configuration on bending moments during eccentric axial compression typical in injurious cadaver spine segment testing. Specific objectives were to create dynamic equilibrium equations for the loads measured inferior to the specimen, experimentally verify these equations, and compare moments from various test configurations using synthetic (rubber) and human cadaver specimens. Dynamic equilibrium equations were developed based on a generic spine testing apparatus. The equations were verified by performing quasistatic and dynamic experiments on a rubber specimen and comparing calculated shear forces and bending moments to those measured using a six-axis load cell. Additional quasistatic and dynamic experiments with various test configurations were performed on rubber and human cadaver cervical spine specimens (consisting of three vertebrae and the interconnecting ligaments and intervertebral discs). Calculated shear force and bending moment curves had similar shapes to those measured and the values in the first local minima differed from those measured by 3% and 15%, respectively, in the dynamic test, and these occurred within 1.5 ms of those measured. In the rubber specimen experiments, for the hinge joint (translation constrained), quasistatic and dynamic posterior eccentric compression resulted in flexion ('unexpected') moments. For the slider and hinge joints and the roller joints (translation unconstrained), extension ('expected') moments were measured quasistatically and initial flexion ('unexpected') moments were measured dynamically. In the human cadaver experiments with roller joints, anterior and posterior eccentric compression resulted in extension moments, which were ‘unexpected’ and ‘expected’, for those configurations respectively. The ‘unexpected’ moments were due to the inertia of the superior mounting structures. This study has shown that eccentric axial compression produces ‘unexpected’ moments due to translation constraints at all loading rates and due to the inertia of the superior mounting structures in dynamic experiments. It may be incorrect to assume that bending moments are equal to the product of compression force and eccentricity, particularly where the test configuration involves translational constraints and where the experiments are dynamic. In order to reduce inertial moment artifacts, the mass, and moment of inertia, of any loading jig structures that rotate with the specimen should be minimized to the extent possible. Also, the distance between these structures and the load cell should be reduced.

Keywords: spine, bending moment, test apparatus, artifact, dynamic, cadaver

Introduction (378 words)

The tolerance of the spine to injurious bending moments is used for the evaluation of injury prevention devices, such as airbags, roofs, and seatbelts [1-3]. These tolerance values may be determined through dynamic experiments using segments of the cadaver spine [4-9]. Bending moments are also applied quasistatically in *ex vivo* models to evaluate spine mechanics [10] and to assess surgical implants [11, 12]. Accurate measurement of the applied bending moments in these experiments is essential for the development of optimal injury prevention and treatment strategies for the spine.

In *ex vivo* spine testing, moments are applied using various means. Opposing cables are used to produce force couples [5, 6, 13, 14] or driven shafts with universal joints may be used to apply pure moments [15]. Moments may also be applied dynamically [4] or quasistatically [10-12] using an axial force at an eccentricity to the center of the spine, where the 'expected' moment is the product of force and eccentricity. Loads may be applied with so-called fixed-fixed [7, 9, 16] or fixed-free [4-6] boundary conditions, which refer to the ability of each side of the specimen to translate and/or rotate. Although pure moment test protocols are widely used for quasistatic evaluations of spine mechanics and spine fixation devices [13, 14, 17, 18], eccentric axial compression loads are more relevant to the study of axial injury of the cervical spine where large compressive impacts occur to the head at a location eccentric from the cervical column resulting in spine bending moments superimposed with the axial compression.

Preliminary experiments in our lab demonstrated that quasistatic and dynamic moment application, through eccentric axial compression forces, resulted in 'unexpected' (artifact) moments. Apparatus-induced moment artifacts have previously been reported for pure moment spine testing [19-21]. In addition, in low rate axial loading of the full cervical spine, translational constraint was shown to reduce bending moments [22]. To our knowledge, the static and dynamic influences of apparatus configurations on bending moments of spine segments in eccentric axial compression have not previously been reported. It was thus our overall objective here to evaluate these influences. Specific objectives were to create dynamic equilibrium equations for a generic spine testing apparatus, experimentally verify the equations, and compare moments from various test configurations using synthetic and human cadaver specimens.

Methods (1000 words)

Equation Development

We developed dynamic equilibrium equations for loads measured inferior to a spine specimen that is connected to and being loaded by a generic spine testing apparatus (Fig. 1). The apparatus consisted of a source of compression loading at a horizontal offset to the center of the specimen (defined as the eccentricity, e), two joints, and an additional mass (representing joints, bearings or other connecting elements) connecting the superior casting cup to the source of compression loading. 'Expected' moments for anterior and posterior eccentricities are flexion and extension, respectively.

In this model, three structures were considered to be separate rigid bodies: the superior block (which could be a slide rail) (m_1, Fig. 1B), the connecting plates and casting cup (m_2, Fig. 1C), and the specimen, lower casting cup, and half of the load cell (m_3, Fig. 1D). The following assumptions were made: motion was in the sagittal plane, m_1 translated, m_3 was stationary, the interface between the m_2 and m_3 was a beam-column joint that transmitted loads, while allowing motion at this interface, and eccentricity was constant.

Using planar kinetic equations of motion, the following equations were determined for the compression (C_4) and shear (F_4) forces and the sagittal plane moments (M_4) measured at the centroid of the load cell (Fig. 1E):

$$C_4 = C_1 - m_1 a_{y1} - m_2 a_{y2} \qquad (1)$$

$$F_4 = F_1 + m_1 a_{x1} + m_2 a_{x2} \qquad (2)$$

$$M_4 = -C_1 e + F_1(h_1 + h_2 + h_3) + M_1 + I_2 \alpha_2 + m_1[(a_{y1} e + a_{x1}(h_1 + h_2 + h_3))] + m_2 h_3 a_{x2} \qquad (3)$$

where h_n, m_n and I_n are the height, mass, and moment of inertia of body n and a_{xn}, a_{yn}, and α_n are the horizontal, vertical, and rotational acceleration of body n. C_1, F_1, and M_1 are the compression, shear, and bending moment imparted at the superior edge of the structure. The directionality of these forces and moments is such that, for a posterior eccentricity, the first term in Eq. (3) acts in extension (i.e. the 'expected' direction) and the five remaining terms act in flexion (i.e. the 'unexpected' direction). The first flexion term is the shear force, which would result from a translational constraint. The second flexion term is the bending moment, which would result from a rotational constraint. The third through fifth flexion terms are dynamic; therefore they would result in appreciable flexion moments, depending on the kinematics of the system, only for dynamic loading rates.

By adjusting parameters in these equations, they may be modified to represent various interfaces between the superior casting cup and the actuator. For a roller joint, $m_1 = h_1 = F_1 = M_1 = 0$, resulting in the following equation:

$$M_4 = -C_1 e + I_2 \alpha_2 + m_2 h_3 a_{x2} \qquad (4)$$

where the first, second, and third terms are the ‘compression’, ‘rotational acceleration’, and ‘linear acceleration’ terms, respectively. For the configuration of slider and hinge joints, where m_1 represents the slide rail (as the slide block is fixed to the actuator), and m_2 represents the hinge joint and superior potting, $F_1 = M_1 = 0$, resulting in the following equation:

$$M_4 = -C_1 e + I_2 \alpha_2 + m_1[(a_{y1} e + a_{x1}(h_1 + h_2 + h_3))] + m_2 h_3 a_{x2} \quad (5)$$

For the configuration of a hinge joint, $m_1 = h_1 = M_1 = 0$, resulting in the following equation:

$$M_4 = -C_1 e + F_1(h_2 + h_3) + I_2 \alpha_2 + m_2 h_3 a_{x2} \quad (6)$$

Equation Verification

In order to verify these equations, tests with a roller joint were performed on a cylindrical specimen of rubber (Fig. 2), which was potted in polymethylmethacrylate (PMMA) inferiorly and superiorly. The roller (Fig. 4C) was attached to the upper specimen mount. The rubber specimen was loaded in eccentric compression (posterior eccentricity of 2.2 cm), under displacement control (8 cm displacement) using a servohydraulic materials test system (model 8874, Instron Corporation, Canton MA) at quasistatic (5 mm/s) and dynamic (0.4 m/s) rates. Six-axis loads inferior to the specimen and horizontal accelerations of the superior mounting structures were recorded at 50 kHz (Fig. 2). The mass of superior mounting structures was 1.44 kg, the vertical distance from the centroid of the load cell to point A was 12.58 cm, and the moment of inertia of m_2 about point A was estimated as 0.00387 kg m^2 (Fig. 1C). The rotational acceleration was approximated as the linear acceleration multiplied by the distance from the point of acceleration measurement to the point where the actuator contacted the roller. As verifications of Eq. 2 and 3, the measured and calculated shear forces and bending moments were compared. For this configuration, Eq. 3 is reduced to Eq. 4 and Eq. 2 is reduced to the following:

$$F_4 = m_2 a_{x2} \quad (7)$$

<u>Test Configuration Comparisons</u>

Synthetic Specimens

The apparatus configurations that were tested were those of a hinge joint (Fig. 4A), a linear slider and a hinge joint (Fig. 4B), and a urethane roller (Fig. 4C) (Table 1). The same rubber specimen was loaded in eccentric axial compression, with a posterior eccentricity of 2.2 cm at quasistatic (5 mm/s) and dynamic (0.4 m/s) rates while loads were measured inferior to the specimen with the six axis load cell.

Human Cadaver Specimens

Sixteen specimens were impact tested using a roller configuration, which have previously been described (Table 1) [4]. Specimens consisted of three cervical vertebrae with the interconnecting spinal ligaments and intervertebral discs. Roller joints (model CCF-1-S, McGill Manufacturing, Valparaiso IN) were fixed at an initial anterior or posterior eccentricity equivalent to the anterior/posterior depth of the middle vertebral body (average 2.8 cm), measured from the centroid of the inferior intervertebral disc. Specimens were tested dynamically using a custom-manufactured high rate materials test system (MTS Systems Corporation, Eden Prairie MN) with a Haversine velocity profile and an ideal pulse width of 16 ms. Six-axis loads inferior to the specimen were recorded (Model 4526, Denton ATD, Rochester Hills, MI).

Data Analysis

Loads and accelerations were low-pass filtered (fourth order, zero phase, cutoff 1 kHz). Loads were transformed from the centroid of the load cell to those at Point C using static equilibrium equations, as previously described [4, 22]. For synthetic samples, this point is where the rubber sample meets the superior edge of the inferior potting material and for cadaver specimens, it is at the centroid of the inferior intervertebral disc (C_C, F_C, M_C in Fig. 1F). It was appropriate to use static equations for this transformation because the specimen or rubber was assumed to be a rigid body attached to the load cell.

Results (435 words)

<u>Equation Verification</u>

Calculated shear force curves were similar in magnitude and shape to those measured (Fig. 3A, C). Measured and calculated shear forces for the quasistatic test were less than 10 N (Fig 3A). For the dynamic test, although the first peak in calculated shear force was 28% less than that in measured shear force (121 N vs. 168 N), the first local minima was only 3% greater than that in measured shear force (-256 N vs. -264 N). Both of these calculated points occurred within 1.5 ms of the corresponding measured points (Fig. 3C).

Calculated bending moment curves were similar in magnitude and shape to those measured (Fig. 3B, D). For the quasistatic test, the peak measured and calculated moments were -7 and -4 Nm, respectively; calculated moments were underestimated due to the assumption of constant eccentricity, as the roller joint allowed eccentricity to increase over time. For the dynamic test, although the first peak in calculated moment was underestimated by 79% (3 Nm vs. 14 Nm), the first local minima was only 15% greater than that in measured moment (-34 Nm vs. -36 Nm). Both of these points occurred within 0.1 ms of the corresponding measured points (Fig. 3D). For the quasistatic and dynamic tests, the compression and linear acceleration terms (Eq. 4) dominated the moment responses, respectively (Fig. 3B, D).

Test Configuration Comparisons

Synthetic Specimens

Posterior eccentric compression resulted in flexion ('unexpected') moments for the hinge joint configuration for both quasistatic and dynamic tests (Fig. 4D, G). For these conditions, substantial shear forces were measured (peak 410 N and 693 N for quasistatic and dynamic tests, respectively). For the configuration with slider and hinge joints, extension moments were measured in the quasistatic test (Fig. 4E) with low shear forces (peak 30 N). In the dynamic test, 'unexpected' flexion moments were measured during the initial compression, followed by extension moments (Fig. 4H). The peak shear force was 541 N. For the roller configuration, extension moments were measured for the quasistatic test (Fig. 4F) with low shear forces (peak 6 N). For the dynamic test, 'unexpected' flexion moments were measured during the initial compression, followed by extension moments (Fig. 4I). The peak shear force was 264 N.

Human Cadaver Specimens

Posterior eccentric compression applied to cadaver specimens resulted in extension ('expected') moments (Fig. 5A, C, E). Anterior eccentric compression resulted in extension ('unexpected') moments during the initial compression, followed by flexion moments (Fig. 5B, D, F). These trends were observed for all specimens. Average peak axial compression forces were 3472 (SD 987) N and 766 (SD 346) N for the posterior and anterior eccentric tests, respectively.

Discussion (704 words)

This study evaluated the static and dynamic effects of various test configurations on bending moments in eccentric axial compression of synthetic and cadaveric spine specimens. Dynamic equilibrium equations were created and verified using synthetic specimens. Measured bending moments were compared between various test configurations with translation constrained and unconstrained using synthetic and cadaveric spine specimens. Eccentric axial compression was shown to produce 'unexpected' moments due to translation constraints, quasistatically and dynamically, and, additionally, due to the inertia of the superior mounting structures, dynamically.

Translational constraint in the test apparatus (i.e. hinge joint) led to quasistatic and dynamic shear forces, which acted to produce a moment that opposed the 'expected' moment. Moments measured in spine segment testing can be significantly altered due to translational constraints and these differences may be of clinical interest, due to the association between constraint and the risk of injury to the spine [22, 23] and spinal cord [23].

Linear and rotational inertia of the superior mounting structures led to dynamic shear forces (observed with the hinge and slider joints and with the roller joint), which were not seen in quasistatic tests, that acted to produce a moment that opposed the 'expected' moment. For the synthetic specimen, the linear acceleration term (third term in Eq. 4) dominated the measured moment and this term contains variables for the mass of the superior mounting structures and the height of these structures above the point of load measurement. Inertial artifacts were greater for the hinge and slider configuration than for the roller configuration and this may be due to the extra mass of the slider accelerating separately from the superior mounting structures. 'Unexpected' moments were produced for the anterior eccentric configuration in the human cadaver experiments but not for the posterior eccentric configuration. For both configurations, the inertia of the superior mounting structures produced shear forces [4] and ‘unexpected’ moments (second and third terms in Eq. 4). However, in the Carter *et al.* study, anterior loading configuration was associated with much lower axial forces than the posterior loading configuration. Therefore, for anterior loading, the inertial terms contributed a larger proportion of the total moment and ‘unexpected’ moments resulted. For posterior loading, the inertial terms had lower relative contributions to the total moment and ‘expected’ moments were produced. In order to reduce inertial moment artifacts in dynamic studies, efforts should be focused on reducing the mass and moment of inertia of the superior mounting structures and on reducing the vertical distance between the center of mass of these structures and the point of load measurement.

The limitations of this study include simplifying assumptions that were made in the development of the dynamic equilibrium equations. These include that motion occurred only in the sagittal plane, eccentricity was constant, the specimen was considered to be a stationary rigid body, and that the accelerations measured at the edge of the superior mounting structures reflected horizontal acceleration at the center of mass and that rotational acceleration could be approximated based on this linear acceleration. Despite these simplifying assumptions, calculated shear forces and bending moments compared well to those measured for the synthetic specimen tested in quasistatic and dynamic test conditions. In addition, a rubber specimen was used, which differs from the cadaveric cervical spine in terms of its energy absorption characteristics, shape, and material properties. The height and diameter of the rubber specimen (55 mm and 45 mm, respectively) were similar to those of a three-vertebra osteoligamentous segment of the cervical spine [24] and the dynamic axial stiffness of the rubber specimen in the roller configuration (100 kN/m) was similar to that of the cadaver spine (113 ± 69 kN/m) [4].

This study has shown that quasistatic and dynamic testing of spine segments are susceptible to moment artifacts. This study highlights that it may be inaccurate to assume that bending moments are equal to the product of compression force and eccentricity, particularly where the test configuration involves translational constraints and where the experiments are dynamic. Caution should be used in interpreting the magnitudes and directions of moments in these cases. In order to reduce inertial moment artifacts, the mass, moment of inertia, and distance from any structures that rotate with the specimen to the load cell should be reduced.

Table 1: Summary of experiments performed. The test configuration that was used to verify the dynamic equilibrium equations is indicated with an *.

Test Configurations	Specimen Type		Translation
	Synthetic (quasistatic & dynamic)	Human Cadaver (dynamic)	
Hinge joint	X		Constrained
Hinge & slider joints	X		Unconstrained
Roller joint	X*	X	Unconstrained

Figure Captions

Figure 1: A) Overall free-body diagram. B-D) Free body diagrams for m_1, m_2, and m_3, respectively. E) Orientation of the load cell outputs indicating the positive force and moment directions for those presented in Figure 3 (F_4 shear force, anterior positive; M_4 bending moment, flexion positive). F) Free-body diagram for calculating the loading environment at point C (synthetic specimens: where the specimen meets the top of the inferior potting material; cadaver specimens: the centroid of the inferior intervertebral disc). Positive force and moment directions for those presented in Figures 4-5 are indicated by C_C (axial force, compression positive), F_C (shear force, anterior positive), and M_C (bending moment, flexion positive).

Figure 2: Photograph of the roller test configuration with the neoprene spring rubber specimen (durometer rating 75A, diameter 4.45 cm, height 5.5 cm, McMaster Carr) potted in PMMA and the accelerometer (model 355B02, PCB Piezotronics, Depew NY) used to measure horizontal accelerations of the superior mounting structures. Six-axis loads were recorded inferior to the specimen (model 4366, Denton ATD, Rochester Hills MI).

Figure 3: Calculated and measured anteroposterior shear force at the load cell (F_4: anterior positive) for the quasistatic (A) and dynamic (C) test with the roller configuration. Shear forces for the dynamic test with the roller configuration are the result of dynamic terms: mass and horizontal acceleration of the structures moving with the specimen (Eq. 7). Calculated and measured sagittal moment at the load cell (M_4: flexion positive) for the quasistatic (B) and dynamic (D) test with the roller configuration. The three terms of the calculated moment are also shown: compression term, linear acceleration term, and rotational acceleration term (Eq. 4).

Figure 4: Photographs of the hinge (part number 4388 80/20 Inc., Columbia City IN) (A), linear slider (model HRW 35CA, THK, Schaumburg IL) and hinge (B), and urethane roller (durometer rating 80A, diameter 1.5", McMaster Carr, Elmhurst IL) (C) joints. For posterior eccentric compression loading, extension moments are 'expected.' Axial force (C_C: compression positive) and sagittal bending moment (M_C: flexion positive) at the inferior edge of the synthetic specimen for the hinge joint (D, G), hinge and slider joints (E, H), and roller joints (F, I). Plots for the quasistatic tests (5 mm/s: D, E, F) and dynamic tests (0.4 m/s: G, H, I) are shown.

Figure 5: Axial force (C_C: compression positive) and sagittal moment (M_C: flexion positive) at the centroid of the inferior intervertebral disc of the human cadaver specimen for the dynamic compression tests with a roller configuration with posterior eccentricity (A-specimen 14, C-specimen 29, E-specimen 39) and with anterior eccentricity (B-specimen 3, D-specimen 5, F-specimen 7) [4]. The average donor age was 73 yrs (standard deviation 18 yrs), 11 specimens were from female donors and five were from male donors. For posterior eccentric loading, extension moments are 'expected' and for anterior eccentric compression loading, flexion moments are 'expected.' Note that A, C, E and B, D, F have different vertical scales.

Figures

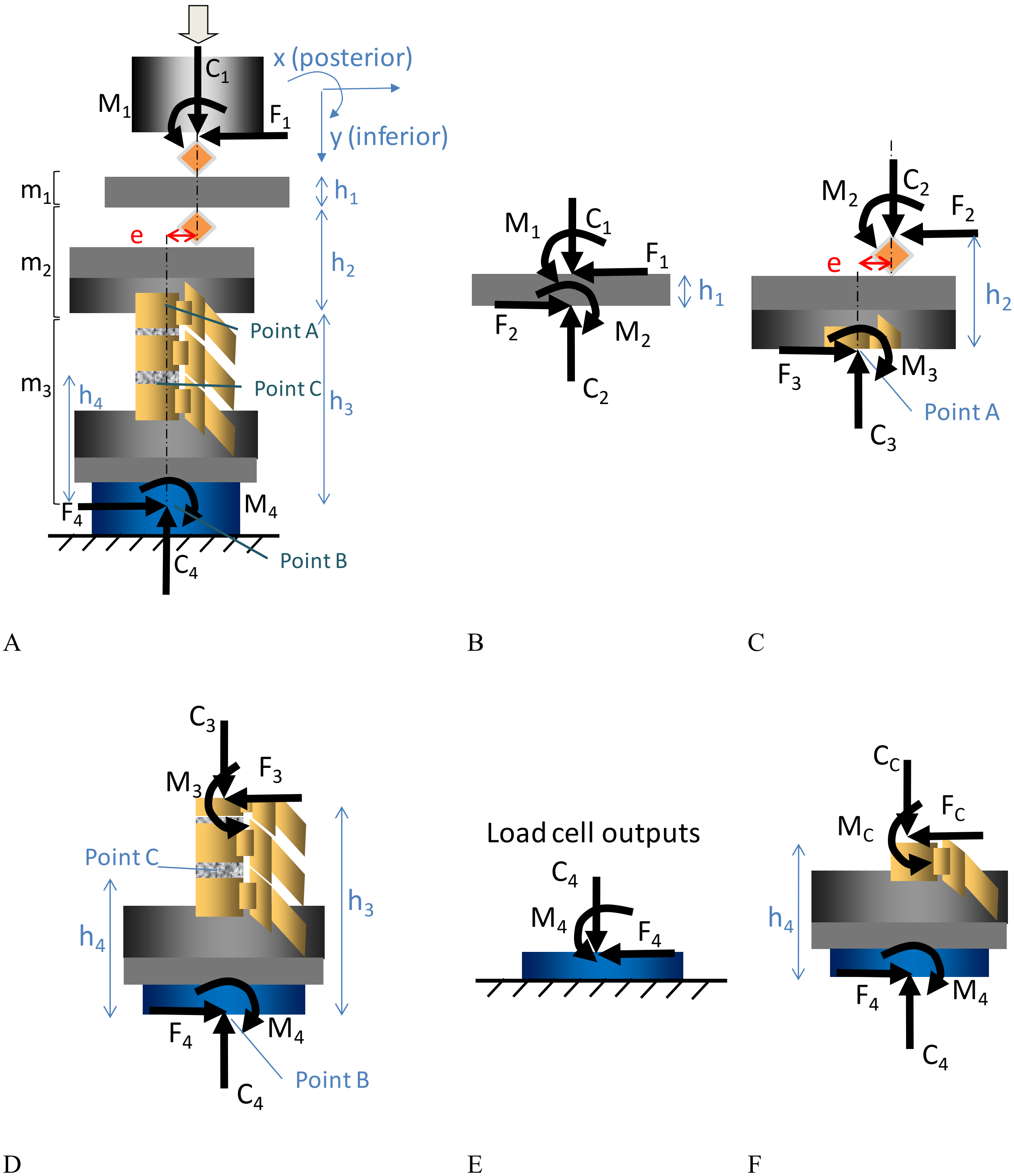

Figure 1

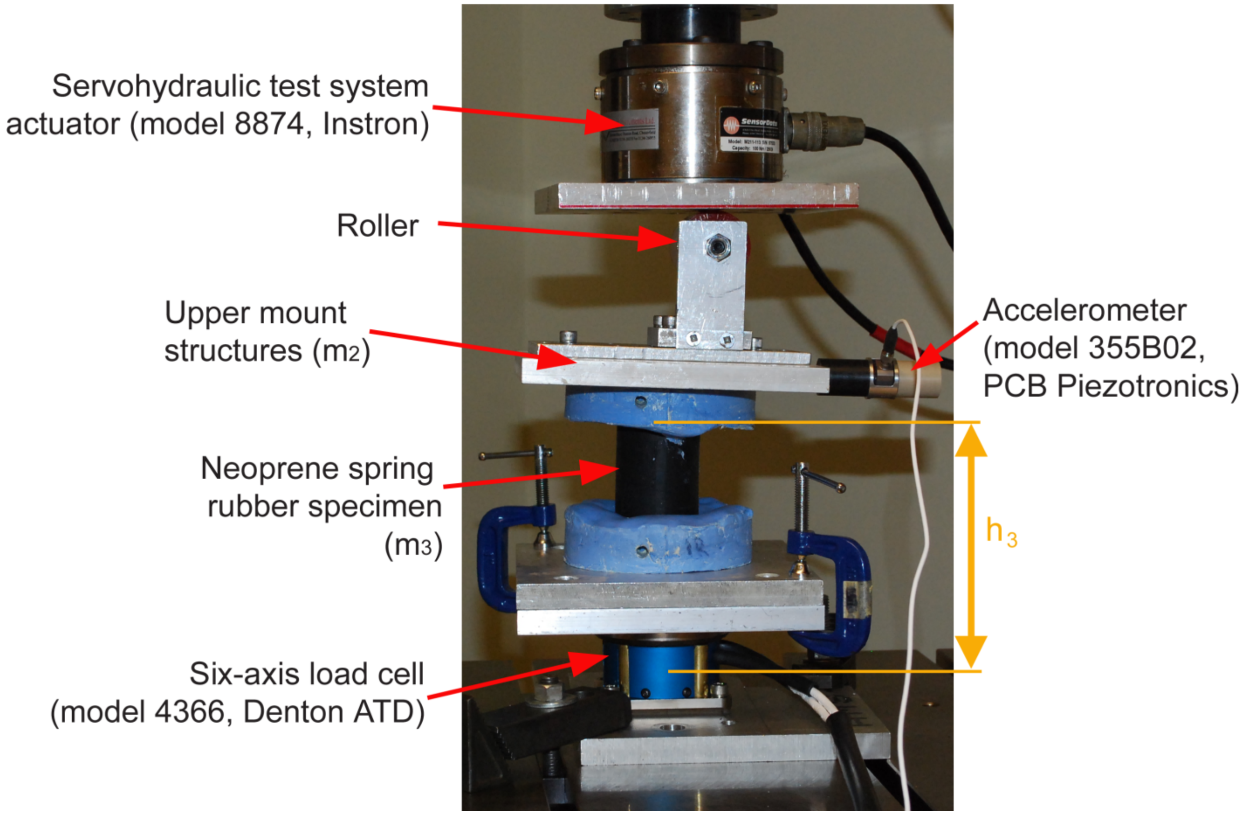
Servohydraulic test system
actuator (model 8874, Instron)
Roller
Upper mount
structures (m2)
Accelerometer
(model 355B02,
PCB Piezotronics)
Neoprene spring
rubber specimen
(m3)
h3
Six-axis load cell
(model 4366, Denton ATD)

Figure 2

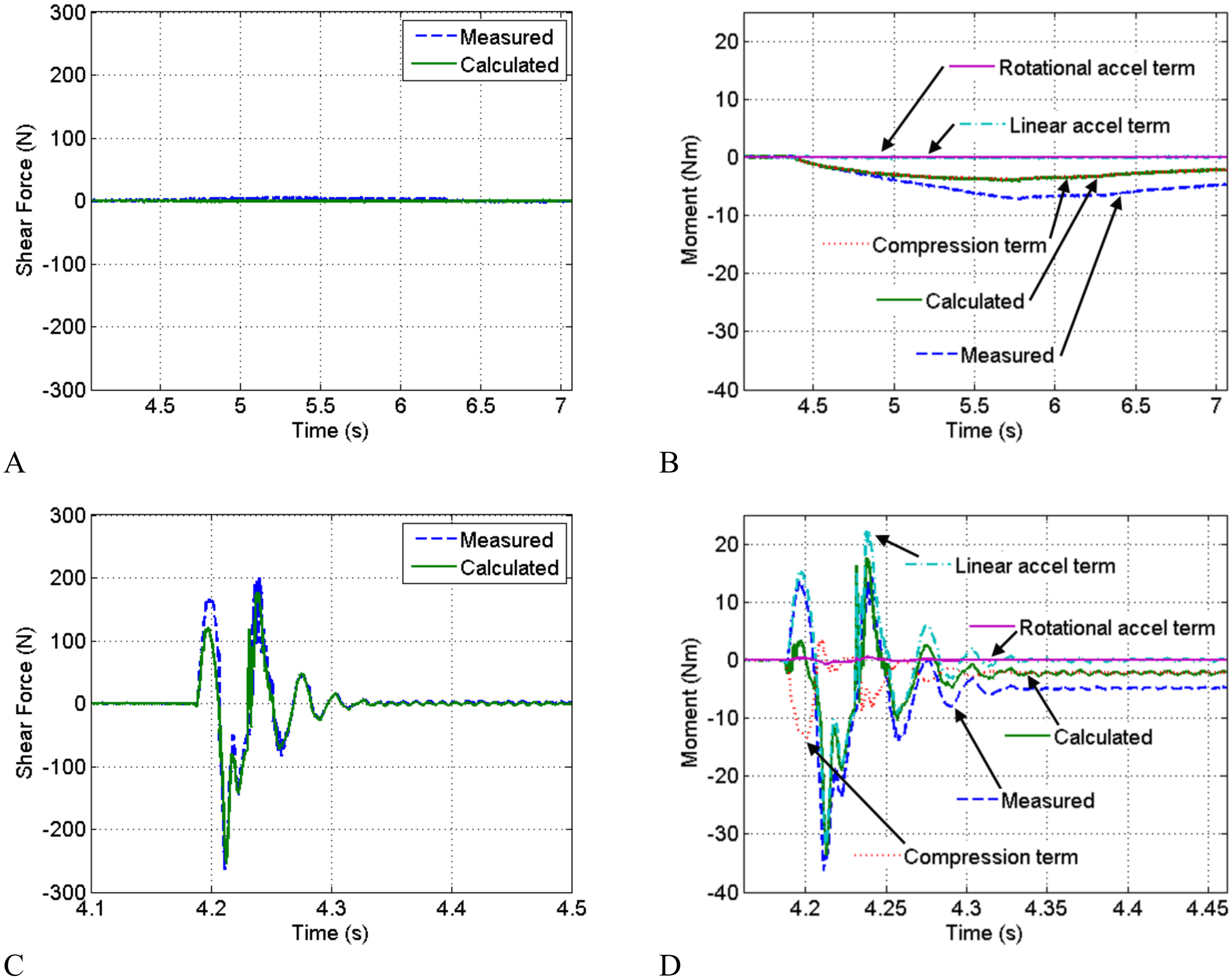

Measured
Calculated
Shear Force (N)
Time (s)
A
Rotational accel term
Linear accel term
Compression term
Calculated
Measured
Moment (Nm)
Time (s)
B
Measured
Calculated
Shear Force (N)
Time (s)
C
Linear accel term
Rotational accel term
Calculated
Measured
Compression term
Moment (Nm)
Time (s)
D

Figure 3

A

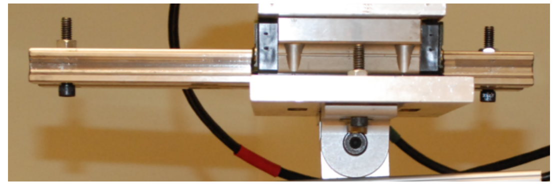

B

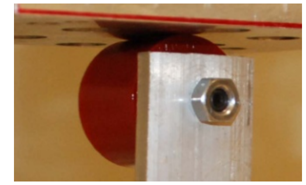

C

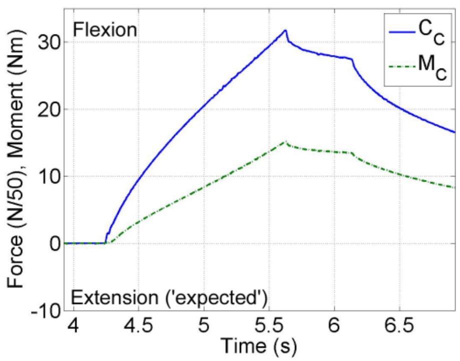

D

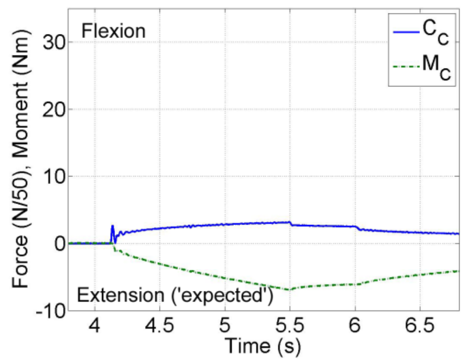

E

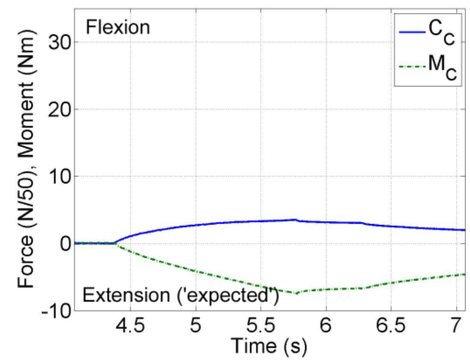

F

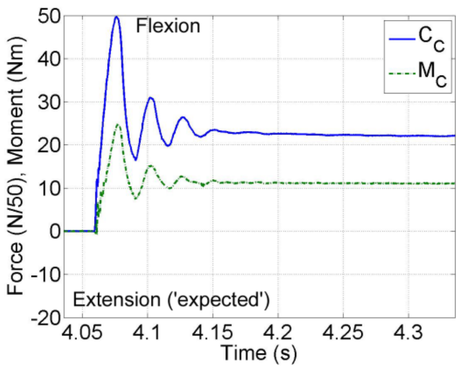

G

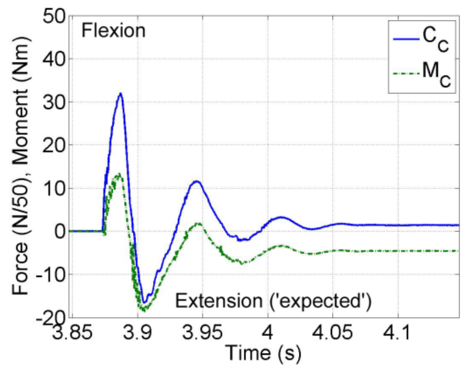

H

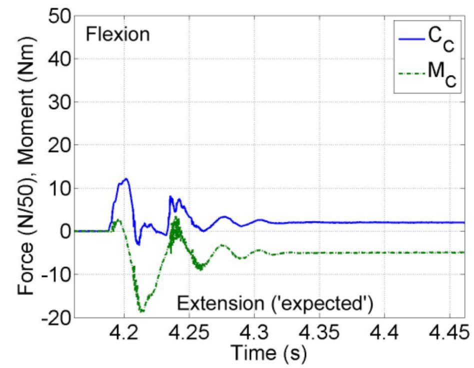

I

Figure 4

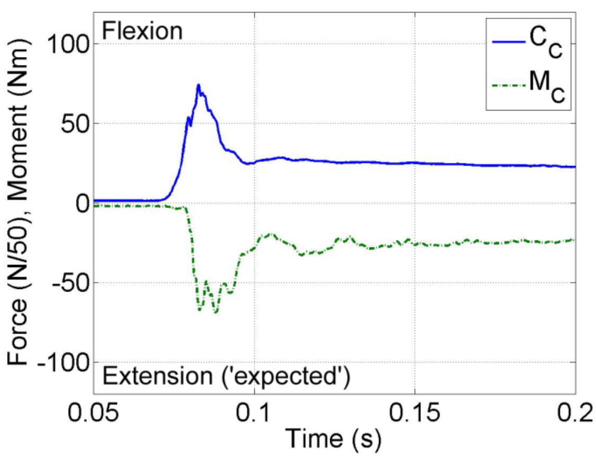

A

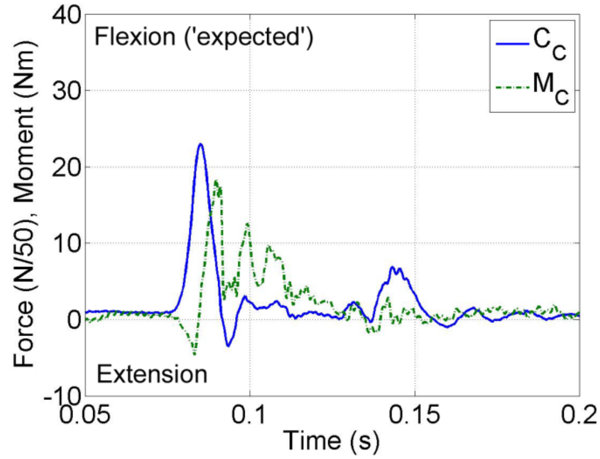

B

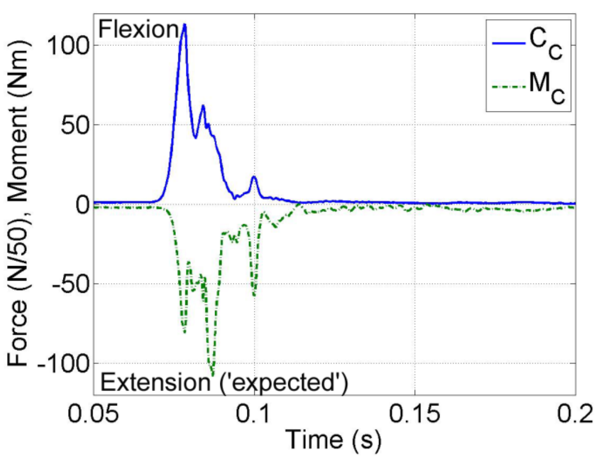

C

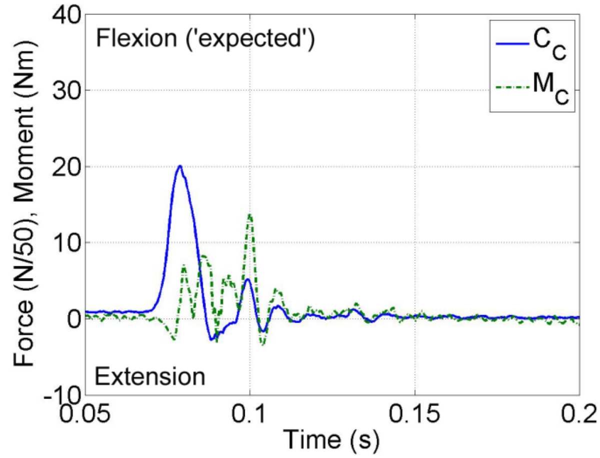

D

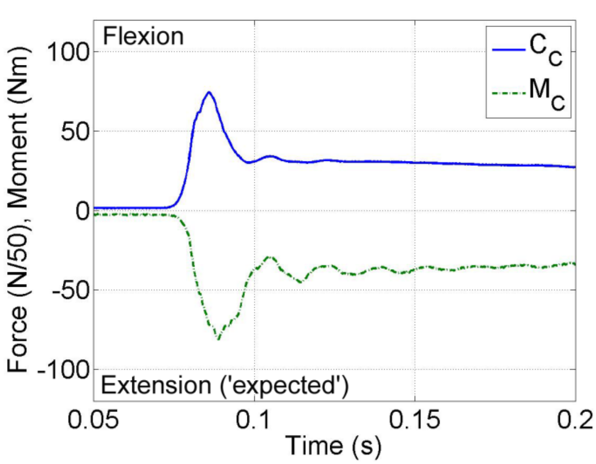

E

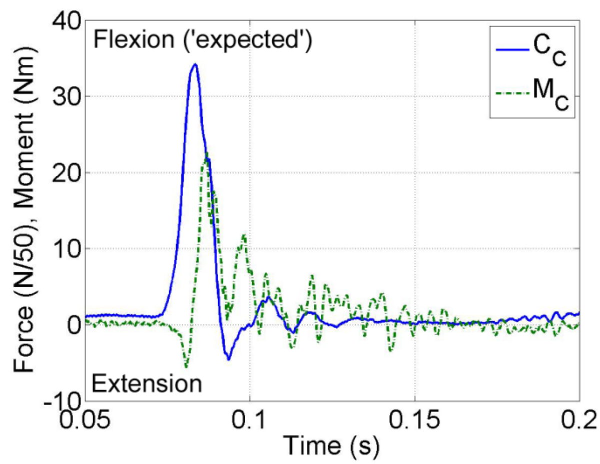

F

Figure 5

Acknowledgements

We are grateful for the financial support from the Natural Sciences and Engineering Research Council and the Canadian Institutes of Health Research.

References

[1] Eppinger, R., Sun, E., Kuppa, S., and Saul, R., 2000, "Supplement: Development of Improved Injury Criteria for the Assessment of Advanced Automotive Restraint Systems - Ii," Technical Report No.
[2] Mertz, H. J., Irwin, A. L., and Prasad, P., 2003, "Biomechanical and Scaling Bases for Frontal and Side Impact Injury Assessment Reference Values," Stapp Car Crash J., 47(pp. 155-88.
[3] Heudorfer, B., Breuninger, M., Karlbauer, U., Kraft, M., and Maidel, J., 2005, "Roofbag - a Concept Study to Provide Enhanced Protection for Head and Neck in Case of Rollover," eds., Washington DC, pp.
[4] Carter, J. W., Ku, G. S., Nuckley, D. J., and Ching, R. P., 2002, "Tolerance of the Cervical Spine to Eccentric Axial Compression," Stapp Car Crash Journal, 46), pp. 441-59.
[5] Nightingale, R. W., Carol Chancey, V., Ottaviano, D., Luck, J. F., Tran, L., Prange, M., and Myers, B. S., 2006, "Flexion and Extension Structural Properties and Strengths for Male Cervical Spine Segments," J Biomech, pp.
[6] Nightingale, R. W., Winkelstein, B. A., Knaub, K. E., Richardson, W. J., Luck, J. F., and Myers, B. S., 2002, "Comparative Strengths and Structural Properties of the Upper and Lower Cervical Spine in Flexion and Extension," J Biomech, 35(6), pp. 725-32.
[7] Crowell, R. R., Shea, M., Edwards, W. T., Clothiaux, P. L., White, A. A., and Hayes, W. C., 1993, "Cervical Injuries under Flexion and Compression Loading," Journal of Spinal Disorders, 6(2), pp. 175-181.
[8] Przybyla, A. S., Skrzypiec, D., Pollintine, P., Dolan, P., and Adams, M. A., 2007, "Strength of the Cervical Spine in Compression and Bending," Spine, 32(15), pp. 1612-20.
[9] Duma, S., Kemper, A. R., and Porta, D. J., 2008, "Biomechanical Response of the Human Cervical Spine," Biomedical Sciences Instrumentation, 44(pp. 135-40.
[10] Schendel, M. J., Wood, K. B., Buttermann, G. R., Lewis, J. L., and Ogilvie, J. W., 1993, "Experimental Measurement of Ligament Force, Facet Force, and Segment Motion in the Human Lumbar Spine," J.Biomech., 26(4-5), pp. 427-438.
[11] Rohlmann, A., Bergmann, G., Graichen, F., and Weber, U., 1997, "Comparison of Loads on Internal Spinal Fixation Devices Measured in Vitro and in Vivo," Med.Eng.Phys., 19(6), pp. 539-546.
[12] Flamme, C. H., Von Der Heide, N., Heymann, C., and Hurschler, C., 2006, "Primary Stability of Anterior Lumbar Stabilization: Interdependence of Implant Type and Endplate Retention or Removal," Eur Spine J, 15(6), pp. 807-18.
[13] Panjabi, M. M., 1988, "Biomechanical Evaluation of Spinal Fixation Devices: I. A Conceptual Framework," Spine, 13(10), pp. 1129-1134.
[14] Panjabi, M. M., Abumi, K., Duranceau, J., and Crisco, J. J., 1988, "Biomechanical Evaluation of Spinal Fixation Devices: Ii. Stability Provided by Eight Internal Fixation Devices," Spine, 13(10), pp. 1135.
[15] Goertzen, D. J., Lane, C., and Oxland, T. R., 2004, "Neutral Zone and Range of Motion in the Spine Are Greater with Stepwise Loading Than with a Continuous Loading Protocol. An in Vitro Porcine Investigation," J Biomech., 37(2), pp. 257-61.
[16] Shea, M., Edwards, W. T., White, A. A., and Hayes, W. C., 1991, "Variations of Stiffness and Strength Along the Human Cervical Spine," Journal of Biomechanics, 24(2), pp. 95-107.
[17] Niosi, C. A., Zhu, Q. A., Wilson, D. C., Keynan, O., Wilson, D. R., and Oxland, T. R., 2006, "Biomechanical Characterization of the Three-Dimensional Kinematic Behaviour of the Dynesys Dynamic Stabilization System: An in Vitro Study," Eur Spine J., 15(6), pp. 913-22. Epub 2005 Oct 11.
[18] Maak, T. G., Ivancic, P. C., Tominaga, Y., and Panjabi, M. M., 2007, "Side Impact Causes Multiplanar Cervical Spine Injuries," J Trauma., 63(6), pp. 1296-307.

[19] Eguizabal, J., Tufaga, M., Scheer, J. K., Ames, C., Lotz, J. C., and Buckley, J. M., 2010, "Pure Moment Testing for Spinal Biomechanics Applications: Fixed Versus Sliding Ring Cable-Driven Test Designs," J Biomech, 43(7), pp. 1422-5.
[20] Gedet, P., Thistlethwaite, P. A., and Ferguson, S. J., 2007, "Minimizing Errors During in Vitro Testing of Multisegmental Spine Specimens: Considerations for Component Selection and Kinematic Measurement," J Biomech., 40(8), pp. 1881-5. Epub 2006 Oct 25.
[21] Cripton, P. A., Bruehlmann, S. B., Orr, T. E., Oxland, T. R., and Nolte, L., 2000, "In Vitro Axial Preload Application During Spine Flexibility Testing: Towards Reduced Apparatus-Related Artefacts," J.Biomech., 33(12), pp. 1559-1568.
[22] Nightingale, R. W., Myers, B. S., Mcelhaney, J. H., Richardson, W. J., and Doherty, B. J., 1991, "The Influence of End Condition on Human Cervical Spine Injury Mechanisms," Society of Automotive Engineers Transactions, Paper 912915, pp. 391-399.
[23] Zhu, Q., Lane, C., Ching, R. P., Gordon, J. D., Fisher, C. G., Dvorak, M. F., Cripton, P. A., and Oxland, T. R., 2008, "Translational Constraint Influences Dynamic Spinal Canal Occlusion of the Thoracic Spine: An in Vitro Experimental Study," J Biomech., 41(1), pp. 171-9. Epub 2007 Aug 20.
[24] Chancey, V. C., Nightingale, R. W., Van Ee, C. A., Knaub, K. E., and Myers, B. S., 2003, "Improved Estimation of Human Neck Tensile Tolerance: Reducing the Range of Reported Tolerance Using Anthropometrically Correct Muscles and Optimized Physiologic Initial Conditions," Stapp Car Crash Journal, 47(pp. 135-53.